

Channel Analysis for 3.5 GHz Frequency in Airport

A. S. Macedo, T. A. Costa, E. M. C. Matos, L. E. C. Eras, J. P. L. Araújo, P. V. G. Castellanos and F. J. B. Barros

Abstract—This letter presents an analysis of the radio propagation channel based on measurements at the 3.5 GHz frequency. The measurement campaigns were carried out inside the Val-de-Cans airport using line-of-sight (LOS) transmissions. First, the channel small-scale dispersion parameters were extracted through channel probing and the results are similar to those obtained by ITU-R P.1238 for the bands below 15 GHz considering commercial indoor environments as well as for those using the 3.5 GHz band in outdoor environments utilizing WiMax OFDM-256 signals. Then, the floating-intercept (FI) and close-in (CI) models are applied and analyzed to evaluate the received signal behavior for co-polarized and cross-polarized antennas. The results show that the CI path loss exponent values are close to the free space propagation loss model, while the FI model provides a lower root mean square error (RMSE) to the measured data. The results show that the FI and CI models are suitable for large-scale indoor propagation loss modeling for 5G networks with a frequency of 3.5 GHz.

Index Terms—Frequency of 3.5 GHz, Airport, Channel Sounding, Small and Large Scale, Co and Cross Polarized.

I. INTRODUCTION

There are several studies in the literature on different frequency bands as alternatives for the new fifth generation (5G) mobile network [1]–[3]. The 5G will cover the frequency spectrum from around 500 MHz to 100 GHz, with emphasis on frequency bands below 6 GHz or so-called Sub-6 GHz bands [3]. Thus, regulators are moving forward with the process of auctioning the spectrum to be used by 5G. In 2021, the Brazilian regulator, Agência Nacional de Telecomunicações (ANATEL), held the auction of the frequency bands that will be used for the implementation of 5G technology, including the 3.5 GHz band [4]. This increases the expectation that the new technologies will provide telephony services with greater coverage and signal quality, presenting a new scenario in telecommunications, new service experiences and economic impact [5]. The growth of multimedia data stream has created new challenges for the development of wireless access technologies that meet the demands of indoor environments with high traffic, such as bus, rail, port and airport terminals [6]–[9]. In this context, experiments are conducted to characterize

the mobile radio channel to evaluate the signal using predictive propagation loss models that support telecommunication systems projects.

Research can be found in the literature on evaluating path loss as a function of distance indoors [10]–[12] and outdoors [13]. In this path loss evaluation, it is of interest to quantify the loss and analyze important parameters, such as the Path Loss Exponent (PLE). In [6], the authors performed a measurement campaign in a Seoul railroad station and an Incheon international airport at 28 GHz, it was estimated that the PLE was 2.15–2.17 and 2.68–3.03 for LOS and NLOS conditions, respectively. In [7], results of losses in two indoor airports environment in the bands 5 and 31 GHz were reported. The study showed that the PLE has similar characteristics to an internal office environment. Industrial scenarios are also of interest for path loss analysis. In [11] the main Sub-6 GHz bands (3.5, 4.9 and 5.8 GHz) were evaluated, and the obtained PLE was less than 2 (in the case of LOS). Moreover, the loss at 3.5 GHz was lower compared to the other frequencies, suggesting better coverage. In [10], the channel at 4.1 GHz is characterized and parameters such as CI model loss are evaluated (with PLE for LOS and NLOS, 1.96 and 2.72, respectively).

Indoor antenna polarization characteristics are studied in various combinations to evaluate the propagation loss behavior through the radiocommunication channel [10], [12], [14]. Such as [10], measurements are reported using directional horn antennas in the same polarization (V-V and H-H) and in cross polarization (V-H) in LOS and NLOS situations for 8–11 GHz indoors environment. In [12], the "n" approach to evaluate path loss with same-polarization and cross-polarization antennas at 11 GHz is considered, where the PLE ranges from 2.0 to 3.0 for the NLOS case and from 0.36 to 1.5 for LOS.

Another feature of signal propagation in a channel is the multipath between the transmitter (Tx) and receiver (Rx), which affects the channel and can be represented by dispersion parameters such as mean dispersion, mean delay, coherence bandwidth and others [12].

This paper studies the signal propagation at 3.5 GHz with a bandwidth of 60 MHz at Val de Cans International airport in Belém, Pará, Brazil. Small and large-scale parameters are extracted from the measurements. The main contributions are the more detailed analysis of the propagation losses at different antenna polarizations and the extraction of their dispersion parameters by channel sounding.

In the next section, the setup and the measurement campaign are presented. Then, the methodology used to characterize the small and large scale channel and the obtained results are described. Finally, the conclusions are presented.

A. S. Macedo (orcid: 0009-0007-7856-8842), T. A. Costa (orcid: 0000-0002-1679-5878), E. M. C. Matos (orcid: 0000-0003-1800-4619), J. P. L. Araújo (orcid: 0000-0003-3514-0401) and F. J. B. Barros (orcid: 0000-0003-0487-0049) are with the Federal University of Pará, 66075-110 Belém, PA, Brazil. (e-mail: alex.macedo@itec.ufpa.br). L. E. C. Eras (orcid: 0000-0003-2818-6145) is with the Federal University of the South and Southeast of Pará, PA, Brazil and P. V. G. Castellanos (orcid: 0000-0001-5783-301X) is with the Federal Fluminense University, Rio de Janeiro, RJ, Brazil.

This work was supported in partly the Coordenação de Aperfeiçoamento de Pessoal de Nível Superior – Brasil (CAPES)- Finance Code 001. Would like to thank the Computation and Telecommunications Laboratory (LCT) and the Electrical Engineering Post-Graduation Program at Federal University of Pará (UFPA-PPGEE) for its financial support.

Digital Object Identifier 10.14209/jcis.2023.13.

II. SETUP AND MEASUREMENT CAMPAIGN

A. Measurement Setup

The equipment used for the measurement campaign is described below. The Fig.1 illustrates of the transmitting (Tx) and receiving (Rx) systems architecture for the channel. This schematic is described in detail below.

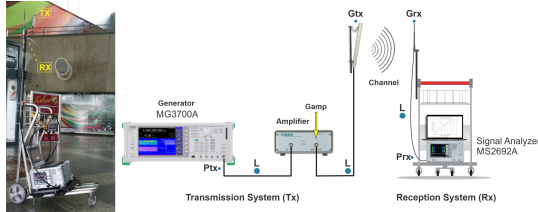


Fig. 1. Transmission (Tx) and Reception (Rx) Systems.

- TX: An Anritsu MG3700A signal generator with a power of -11 dBm was used to transmit the signal, connected to a power amplifier (MilMega AS0204-7B: 2-4GHz-7W) according to the linearity curve, with 46 dB gain at the output. A Hyperlink HG3515P-120 panel antenna with an operating frequency in the range of 3.4 GHz to 3.7 GHz, 120° horizontal aperture, 8° vertical aperture, and gain G_{Tx} of 16 dBi. Therefore, P_{tx} is the value of the amplifier output 35 dBm added to the G_{Tx} 16 dBi, with a value of 51 dBm. The transmitted signal has a bandwidth of 60 MHz. The Tx antenna height was 7.9 meters above the ground.
- RX: A cart was adapted to receive the signal, on which was mounted an omnidirectional receive antenna (Hyperlink HG3505RD-RSP) with an operating frequency range of 3.4-3.6 GHz, with 5 dBi G_{Rx} gain, a horizontal aperture of 360°, a laptop computer, and an MS2692A signal analyzer for data acquisition. The cart's average speed was about 0.87 m/s. Fig.2 shows the radiation pattern of the Tx and Rx antennas [15]. With the signal analyzer, the trigger function was activated to capture raw data in the form of I and Q at a specific moment, for our study case was every second. Subsequently, they are sent to a notebook via a network cable using Matlab software through a script specially coded for this signal analysis methodology. The transmitted signal is captured by the Rx antenna with gain (G_{Rx}), and the I and Q components are allocated in the notebook for post-processing analysis. The received data are in .dgz and .xml format.

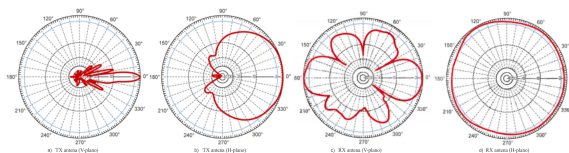


Fig. 2. Radiation Diagrams: a) Vertical Flat Tx Antenna. b) Horizontal Flat Tx Antenna. c) Vertical Flat Rx Antenna. d) Horizontal Flat Rx Antenna.

B. measurement campaign

Measurements were made in the arrivals lounge of Val de Cans International airport in Belém do Pará, Brazil. The Fig.

3 shows the lounge's floor plan, highlighted in yellow, with a 25 m width, 60 m length, and corresponding area of 1.480 m^2 .

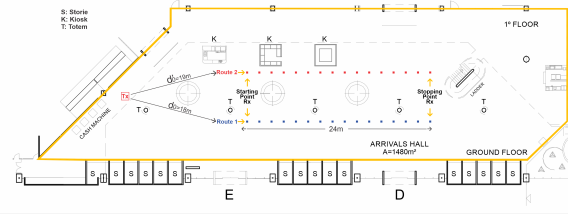


Fig. 3. Floor Plan of the Arrivals Hall

The lounge ceiling is inclined and its height varies from 8 m to 12 m. Inside the lounge have kiosks, stores, and totem-shaped air vents made of iron. The exterior walls are made of concrete columns, glass and a plaster ceiling. The second floor is made of concrete and steel ventilation ducts (see Fig. 4).



Fig. 4. Arrivals Hall and Routes defined for measurements

Two parallel routes, free of obstacles between the start and end points, were chosen to collect the raw data (in dgz and xml formats). They were named Routes 1 (R1) and 2 (R2) with a length of 24 meters and are represented by the blue and red colors, respectively. Data collection was conducted during the night, when the airport shops were closed, and considering the schedules provided by the airlines when passengers passengers were not arriving. Therefore, The environment had a minimum flow of people.

During the measurements, both antenna's polarization was adjusted to collect data with equal and crossed polarizations. The polarization configurations were as follows: Vertical-Vertical (V-V), Horizontal-Horizontal (H-H). The distances between TX and the starting points of routes R1 and R2 are indicated as d_0 e d'_0 in Fig. 3.

III. MODELING AND ANALYSIS OF RESULTS

This section presents channel sounding and analysis of small- and large-scale features.

A. Channel Analysis at 3.5 GHz

The channel analysis is conducted using an orthogonal frequency division multiplexing (OFDM) signal, which consists

of transmitting a wideband signal with multiple narrowband channels [13]. The profiles are obtained by applying the constant false alarm rate (CFAR) method [16], a profile cleanup technique that distinguishes multipath components from noise components [17]. The power delay profile (PDP) allows the determination of parameters that characterize wireless channels, such as the mean delay (MD), the delay spread (DS) and the coherence band (B_{CO}). The B_{CO} is defined as the smallest frequency separation at which the autocorrelation of the transfer function reaches a certain value, which in this case was applied to the values 0.9 and 0.7 [18].

The methodology used to determine the small-scale metrics is presented in section III - A1 and section III - A4 describes the path loss models and the results.

1) *Small Scale Channel Dispersion Parameters:* Initially, the PDP of the channel is analyzed to obtain the profiles through the CFAR filtering technique, thereby determining the valid multipath components given by τ . In order to validate the behavior of the delay profiles, the calculated multipaths in the obtained delay profiles were statistically modeled in terms of the set of components reaching the receiver.

2) *Verification step:* to perform the analysis of the mean delay RMS and the mean scattering RMS, the results obtained on the two routes R1 and R2 were verified. These values were evaluated point-to-point for the whole samples, according to the structures present in the environment.

The channel probing technique used to verify the multipath components is described as follows:

- The first multipath component is found at $\tau_0 = 0$. Physically, however, the first component corresponds to the direct beam and is taken at a value of τ greater than zero ($\tau_0 > 0$);
- Subsequent components must also be added to τ_0 . That is, $\tau_i + \tau_0$.
- The value of the first component's delay is given by the expression $\tau = d/C$, where τ , d and C representing the delay, distance, and speed of light, respectively.

Fig. 5 presents the power profiles of the given delay in dB, relative to the delay time in nanoseconds (ns). Point 20 on route R2 was selected to verify and understand the multipath components.

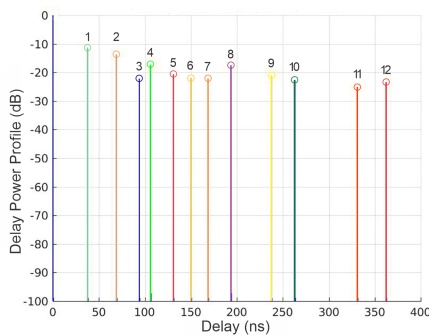


Fig. 5. Delay Power Profile Components

Fig. 6 corresponds to the scenario and the possible paths taken by the rays between Tx and Rx. These rays are correlated according to each point in Fig. 5.

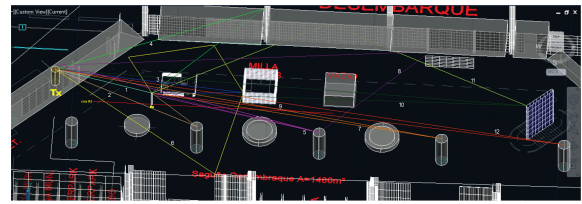


Fig. 6. 3D simulation of multipath rays in AutoCad

Each multipath point is identified by a color and numbered. Point number 1 (cyan) identifies the first component, representing the direct ray in the time of 37.5 ns and at a distance of 29.5 m.

Point 2 (salmon) indicates the profile that arrives with a delay concerning point 1 in 68.35 ns has traveled 50 m. Furthermore, this ray consists of a reflection or diffraction signal from obstacles near Rx. This analysis is also valid for the other points from 3 to 12.

These possible rays validate the measurement campaign on a small scale since the airport spreaders can reproduce the multipath components obtained. Table I contains the values of the small scale scattering parameters for the V-V and H-H polarizations. Therefore, according to Table I, the V-V polarization performs better.

TABLE I
SMALL-SCALE CHANNEL DISPERSION PARAMETERS AND COHERENCE BAND

Pol.	Mean Delay (ns)		Delay Spread (ns)	
	Average	Median	Average	Median
VV	R1: 162.1	R1: 87.5	R1: 144.1	R1: 89.50
	R2: 98.30	R2: 89.4	R2: 77.00	R2: 70.00
HH	R1: 110	R1: 98.00	R1: 90.00	R1: 52.40
	R2: 104.5	R2: 98.50	R2: 95.00	R2: 57.50
Pol.	Coherence Band 0.9 (KHz)		Coherence Band 0.7 (KHz)	
	Average	Median	Average	Median
VV	R1: 7.50	R1: 7.20	R1: 4.50	R1: 4.75
	R2: 6.90	R2: 6.80	R2: 4.20	R1: 4.20
HH	R1: 8.00	R1: 8.20	R1: 4.47	R1: 4.50
	R2: 8.20	R2: 8.10	R2: 4.47	R1: 4.30

3) *Analysis and Results Stage:* Post-processing of the 64.000 raw data consisted of determining the phase (I) and quadrature signal (Q) for each OFDM symbol and generating the data for channel dispersion analysis and coherence band determination. The data was captured continuously with a sampling rate of 1 second.

First, the parameters MD and DS were observed. It was found that for routes R1 and R2, the values of MD and DS in V-V show, on average, a greater delay compared to H-H polarization. These values in R1 for V-V were 162.1 ns and 144 ns, respectively, and for R2, the values were 98.30 ns and 77.00 ns, respectively.

Although the routes were close, they had different values. The results in R2 are justified by the characteristics of this route, being closer to the walls and 1st-floor ceiling, which means the signal is more confined, as seen in Fig. 3.

Regarding the coherence band, a variation of 8 to 12 kHz was obtained for a correlation of 0.9 and 4 to 8 KHz for a correlation of 0.7, according to Fig. 7, respectively. As seen in Table 1, these values are higher for R1 and lower for R2

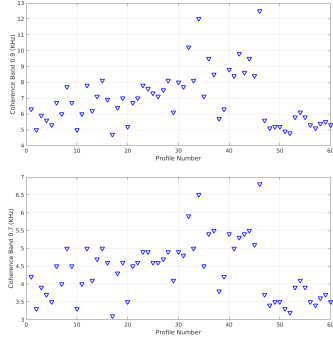


Fig. 7. Coherence Band 90% and 70% for Route 1 V-V

compared to the H-H polarization. The temporal parameters found are in accordance with those evaluated in the works [13], [19], [20].

4) *Analysis and Results on a Large Scale:* Signal analysis and approximation for the LOS condition is performed using the FI, CI, and CIX models, which allow the addition of the parameter for loss due to cross-polarized antennas. These models were chosen because they are applied in the WINNER II standards and mainly in the 3GPP (3rd Generation Partnership Project) standards for the Sub-6 GHz bands, they can be used due to their adequate performance in the mmWave bands for 5G systems [14].

The common model of path loss CI is given by equation (1), which defines the losses due to propagation in free space (FSPL), equation (2), at a distance d_0 of 1 m between Tx and Rx. The PLE or n is the loss coefficient as a function of distance. The CI is calculated by linear regression of the PLE applying the Minimum Mean Square Error (MMSE) technique, which fits to the measured data by finding the minor error using a physical anchor point. The term $X\sigma^{CI}$ is a Gaussian random variable with a mean of 0 and a standard deviation σ in dB. [14].

$$PL^{CI} = FSPL + 10n_{(VV)}\log_{10}(d/d_0) + X\sigma^{CI} \quad (1)$$

where $d \geq d_0$; when $d_0 = 1m$.

$$FSPL(f, d_0) = 10\log_{10}(4\pi d_0/\lambda)^2 \quad (2)$$

The PLE factors differ depending on the type of environment and its polarization [14]. Therefore, the CI method of equation (1) is applied for co-polarization H-H, where the PLE (n_{HH}) is the loss factor with the data in H-H. This is how the PL^{CIHH} is determined [10].

The CIX model was applied to the V-H and H-V polarizations. This resulted in the determination of two new PLE factors (n_{VH} e n_{HV}). In addition, a cross polarization discrimination factor called XPD was also added. This factor is a constant and is determined via MMSE and expressed in dB. The expressions are given by equation (3) [10].

$$PL^{CIX} = FSPL + 10n_{(VHouHV)}\log_{10}(d/d_0) + XPD + X\sigma^{CIX} \quad (3)$$

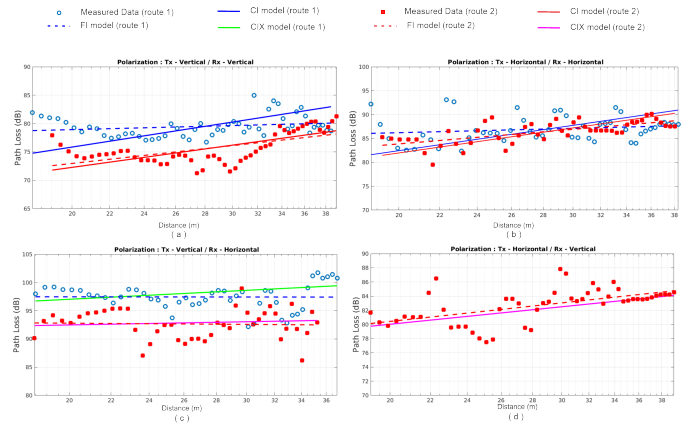


Fig. 8. Path Loss in Vertical-Vertical Polarization (a); Path Loss in Horizontal-Horizontal Polarization (b); Path Loss in Vertical-Horizontal Polarization (c); Path Loss in Horizontal-Vertical Polarization (d)

Another model considered is the FI, which requires two parameters, one for the offset of the measured path loss, α , and coefficient b which depends on the distance, equation (4) presents the FI model [14]:

$$PL^{FI} = \alpha + 10\beta\log_{10}(d) + X\sigma^{FI} \quad (4)$$

Two routes (R1 and R2) were analyzed in the environment. For each route measurements were made considering the same V-V and H-H polarizations and the V-H and H-V cross-polarizations, then FI, CI, and CIX models were applied. Furthermore, the PLE parameters were determined and the RMSE and standard deviation (σ) values were calculated to verify the performance of the models. The Fig. 8 in blue represent R1 and red R2.

Fig. 8 (a) contains the measured data and model fits for V-V polarization. For the CI model, PLE values 2.50 and 2.22 were obtained for R1 and R2, respectively. The blue measured data in R1 show few variation in the first meters. However, after 30 meters, the loss increase considerable since R1 passes through a wide space region and suffers less interposition of signals. For the FI model, the β was 0.40 and 1.78 in R1 and R2, respectively, as found in [6], [11]. It was also observed that the losses in R1 are larger than in R2 because R1 is located in a larger space that is farther from the side walls according to Fig. 3. In contrast, R2 is near an enclosed space between the first floor and the concrete ceiling, as seen in Fig. 3, making the signal more confined. Furthermore, the RMSE is smaller for the FI model, presenting a good approximation with the measured data.

For H-H co-polarization, illustrated in Fig. 8 (b), the values of PLE, 3.01 and 2.8, were obtained for the CI model loss in R1 and R2, respectively, as found in [6], [11]. Note that these values are close due to the radiation diagram of the TX antenna, which has greater coverage for horizontally positioning. The FI model had the lowest standard deviation and RMSE.

Fig. 8 (c), presents the results in V-H. Note that as the distance increases, there is no significant variation in the loss up to 25 m, but after 28 m, the losses tend to vary. Note the negative β value in FI in both routes, low values found in [10]. This behavior is related to the propagating wave in TX that had vertical electromagnetic components and now has horizontal components. Thus, there is a gain in signal transmission due to polarization mismatch loss reduction [18].

In Fig. 8 (d), the H-V loss results are presented. In this case, the PLE value was 1.48. Note that loss tends to increase from 26 meters. Losses in H-V are less compared to V-H. This similarity was also observed in [12].

All the model's parameters obtained are listed in Table II.

TABLE II
PATH LOSS PARAMETERS OF THE MODELS CI, CIX E FI EM 3.5 GHZ.

LOSS OF PATH OF THE MODELS CI e CIX				
Pol.	PLE (n)	σ (dB)	RMSE	XPB (dB)
V-V	R1: 2.50	R1: 2.71	R1: 2.69	-
	R2: 2.22	R2: 2.21	R2: 2.19	
V-H	R1: 0.90	R1: 2.44	R1: 2.54	R1: 21
	R2: 0.32	R2: 2.62	R2: 2.59	R2: 23
H-H	R1: 3.00	R1: 3.51	R1: 3.48	-
	R2: 2.97	R2: 2.03	R2: 2.01	
H-V	R2: 1.48	R2: 1.99	R2: 2.04	18
LOSS OF PATH OF THE MODEL FI				
Pol.	α	β (dB)	σ (dB)	RMSE
V-V	R1: 73.67	R1: 0.40	R1: 1.81	R1: 1.80
	R2: 49.70	R2: 1.78	R2: 2.17	R2: 2.15
V-H	R1: 97.68	R1: -0.017	R1: 2.30	R1: 2.28
	R2: 94.32	R2: -0.11	R2: 2.59	R2: 2.56
H-H	R1: 79.51	R1: 0.51	R1: 2.67	R1: 2.64
	R2: 61.33	R2: 1.73	R2: 1.72	R2: 1.70
H-V	R2: 61.10	R2: 1.48	R2: 1.99	R2: 1.97

IV. CONCLUSIONS

In this paper, measurements from an airport scenario were analyzed to examine channel parameters at both small and large scales. In the small-scale analysis, an average deviation of 144 and 77 ns was found for R1 and R2, respectively, in V-V, getting better performance compared to H-H. Regarding the coherence band, for the 0.9 correlation, there was a variation between 8 - 12 KHz, and for the 0.7 correlation, the variation was 4 - 8 KHz. For a large-scale analysis, two propagation loss models, CI and FI, were compared. The results show that the PLE ranges from 2.22 to 2.50 in V-V and from 2.9 to 3 in H-H. The FI model has a lower RMSE than the CI model, showing better performance. Consequently, it was found that there is agreement between this work and the studies found in the literature for other frequencies in large indoor spaces. These measurement results and methodology will be beneficial to the development of channel models in Sub-6 GHz bands.

REFERENCES

[1] M. U. Sheikh, L. Mela, N. Saba, K. Ruttik, and R. Jantti, "Outdoor to indoor path loss measurement at 1.8ghz, 3.5ghz, 6.5ghz, and 26ghz commercial frequency bands," in 2021 24th International Symposium on Wireless Personal Multimedia Communications (WPMC). IEEE, dec 2021. [Online]. Available: <https://doi.org/10.1109/wpmc52694.2021.9700427>

[2] Y. Yu, W.-J. Lu, T.-T. Liu, W.-H. Zeng, Y. Liu, and H.-B. Zhu, "Person Density Dependency on Path Loss and Root Mean Square Delay Spread for Smart Office Scenarios," IEEE Internet Things J., vol. 9, no. 13, pp. 11190-11202, jul 2022. [Online]. Available: <https://doi.org/10.1109/jiot.2021.3125750>

[3] J. Rischke, P. Sossalla, S. Itting, F. H. P. Fitzek, and M. Reisslein, "5G Campus Networks: A First Measurement Study," IEEE Access, vol. 9, pp. 121786-121803, 2021. [Online]. Available: <https://doi.org/10.1109/access.2021.3108423>

[4] ANATEL, "Agência Nacional de Telecomunicações," <https://www.gov.br/anatel/pt-br>.

[5] G. Smail and J. Weijia, "Techno-economic analysis and prediction for the deployment of 5G mobile network," in 2017 20th Conference on Innovations in Clouds, Internet and Networks (ICIN). IEEE, mar 2017. [Online]. Available: <https://doi.org/10.1109/icin.2017.7899243>

[6] J. Lee, J. Liang, J.-J. Park, and M.-D. Kim, "Directional path loss characteristics of large indoor environments with 28 GHz measurements," in 2015 IEEE 26th Annual International Symposium on Personal, Indoor, and Mobile Radio Communications (PIMRC). IEEE, aug 2015. [Online]. Available: <https://doi.org/10.1109/pimrc.2015.7343663>

[7] D. W. Matolak, M. Mohsen, and J. Chen, "path loss at 5 GHz and 31 GHz for two distinct indoor airport settings," in 2019 27th European Signal Processing Conference (EUSIPCO). IEEE, sep 2019. [Online]. Available: <https://doi.org/10.23919/eusipco.2019.8902509>

[8] M. A. Mou, M. M. Mowla, and H. B. H. Dutty, "Statistical mmWave Channel Modeling and Characterization in Indoor Airport Environments," in 2019 22nd International Conference on Computer and Information Technology (ICCIT). IEEE, dec 2019. [Online]. Available: <https://doi.org/10.1109/iccit48885.2019.9038494>

[9] J. Kim, C.-S. Kim, J.-Y. Hong, J.-S. Lim, and Y.-J. Chong, "Propagation Characteristics of an Industrial Environment Channel at 4.1 GHz," in 2021 International Conference on Information and Communication Technology Convergence (ICTC). IEEE, oct 2021. [Online]. Available: <https://doi.org/10.1109/ictc52510.2021.9621008>

[10] I. S. Batalha, A. V. R. Lopes, J. P. L. Araújo, F. J. B. Barros, B. L. S. Castro, G. P. S. Cavalcante, and E. G. Pelaes, "Large-Scale Channel Modeling and Measurements for 10GHz in Indoor environments," Int. J. Antenn. Propag., vol. 2019, pp. 1-10, jan 2019. [Online]. Available: <https://doi.org/10.1155/2019/9454271>

[11] K. Zhang, B. Li, X. Tang, D. Wang, and L. Wei, "Path Loss Measurement and Modeling for Industrial Environment," in 2019 IEEE 20th International Conference on High Performance Switching and Routing (HPSR). IEEE, may 2019. [Online]. Available: <https://doi.org/10.1109/hpsr.2019.8808124>

[12] M. Kim, Y. Konishi, Y. Chang, and J. ichi Takada, "Large Scale Parameters and Double-Directional Characterization of Indoor Wideband Radio Multipath Channels at 11 10GHz," IEEE Trans. Antennas Propag., vol. 62, no. 1, pp. 430-441, jan 2014. [Online]. Available: <https://doi.org/10.1109/tap.2013.2288633>

[13] J. V. Gonçalves, "Variabilidade do Sinal, Banda de Coerência eEspalhamento Temporal em Ambiente de Rádio Propagação Móvel em3,5GHz," Master's thesis, Pontifícia Universidade Católica do Rio de Janeiro PUC-RIO, Setembro, 2009.

[14] G. R. Maccartney, T. S. Rappaport, S. Sun, and S. Deng, "Indoor Office Wideband Millimeter Wave Propagation Measurements and Channel Models at 28 and 73 GHz for Ultra Dense 5G Wireless Networks," IEEE Access, vol. 3, pp. 2388-2424, 2015. [Online]. Available: <https://doi.org/10.1109/access.2015.2486778>

[15] C. Ron, "CARACTERIZAÇÃO DO CANAL RÁDIO EM BANDA LARGA NA FAIXA DE 3,5 GHZ EM AMBIENTE URBANO," Ph.D. dissertation, PONTIFÍCIA UNIVERSIDADE CATÓLICA DO RIO DE JANEIRO - PUC-RIO, 2009. [Online]. Available: <https://doi.org/10.17771/pucRio.acad.32622>

[16] L. Scharf, Statistical signal processing : detection, estimation, and time series analysis. Reading, Mass: Addison-Wesley Pub. Co, 1991.

[17] E. Sousa, v.m. Jovanovic, and c. Daigneault, "Delay spread measurements for the digital cellular channel in Toronto," IEEE Trans. Veh. Technol., vol. 43, no. 4, pp. 837-847, 1994. [Online]. Available: <https://doi.org/10.1109/25.330145>

[18] T. Rappaport, Wireless communications : principles and practice. Upper Saddle River, N.J: Prentice Hall PTR, 2002.

[19] ITU-R, "Propagation data and prediction methods for the planning of indoor radiocommunication systems and radio local area networks in the frequency range 300MHz to 100GHz," Rec. ITU-R P.1238-8, July, 2015.

[20] Y. Yoon, J. Kim, and Y. Chong, "Multipath delay characteristic in mm-Wave radio propagation in indoor public area," in 2016 International Conference on Information and Communication Technology Convergence (ICTC). IEEE, oct 2016. [Online]. Available: <https://doi.org/10.1109/ictc.2016.7763342>